Photodiagnosis and Photodynamic Therapy 42 (2023) 103532

Contents lists available at ScienceDirect

Photodiagnosis and Photodynamic Therapy

journal homepage: www.elsevier.com/locate/pdpdt

Comparison of surface-enhanced Raman spectral data sets of filtrate portions of serum samples of hepatitis B and Hepatitis C infected patients obtained by centrifugal filtration

Muhammad Zaman Nawaz [a], Haq Nawaz [a,**], Muhammad Irfan Majeed [a,**], Nosheen Rashid [b,*], Muhammad Rizwan Javed [c], Saima Naz [b], Muhammad Zeeshan Ali [a], Amina Sabir [a], Nimra Sadaf [a], Ali Raza [a], Muhammad Shakeel [a], Zain Ali [a], Imran Amin [d]

[a] Department of Chemistry, University of Agriculture Faisalabad, Faisalabad 38000, Pakistan
[b] Department of Chemistry, University of Education, Faisalabad Campus, Faisalabad 38000, Pakistan
[c] Department of Bioinformatics and Biotechnology, Government College University Faisalabad (GCUF), Faisalabad 38000, Pakistan
[d] PCR Laboratory, PINUM Hospital, Faisalabad 38000, Pakistan

ARTICLE INFO

Keywords:
Surface-enhanced Raman spectroscopy
Hepatitis B
Hepatitis C
Principal component analysis
Partial least square discriminant analysis
Centrifugal filtration

ABSTRACT

Background: Surface-enhanced Raman spectroscopy (SERS) is an efficient technique which has been used for the analysis of filtrate portions of serum samples of Hepatitis B (HBV) and Hepatitis C (HCV) virus.
Objectives: The main reason for this study is to differentiate and compare HBV and HCV serum samples for disease diagnosis through SERS. Hepatitis B and hepatitis C disease biomarkers are more predictable in their centrifuged form as compared in their uncentrifuged form. For differentiation of SERS spectral data sets of hepatitis B, hepatitis C and healthy person principal component analysis (PCA) proved to be a helpful. Centrifugally filtered serum samples of hepatitis B and hepatitis C are clearly differentiated from centrifugally filtered serum samples of healthy individuals by using partial least square discriminant analysis (PLS-DA).
Methodology: Serum sample of HBV, HCV and healthy patients were centrifugally filtered to separate filtrate portion for studying biochemical changes in serum sample. The SERS of these samples is performed using silver nanoparticles as substrates to identify specific spectral features of both viral diseases which can be used for the diagnosis and differentiation of these diseases. The purpose of centrifugal filtration of the serum samples of HBV and HCV positive and control samples by using filter membranes of 50 KDa size is to eliminate the proteins bigger than 50 KDa so that their contribution in the SERS spectrum is removed and disease related smaller proteins may be observed. Principal component analysis (PCA) and partial least square discriminant analysis (PLS-DA) are statistical tools which were used for the further validation of SERS.
Results: HBV and HCV centrifugally filtered serum sample were compared and biomarkers including (uracil, phenylalanine, methionine, adenine, phosphodiester, proline, tyrosine, tryptophan, amino acid, thymine, fatty acid, nucleic acid, triglyceride, guanine and hydroxyproline) were identified through PCA and PLS-DA. Principal component analysis (PCA) and partial least square discriminant analysis (PLS-DA) were used as a multivariate data analysis tool for the diagnosis of the characteristic SERS spectral features associated with both types of viral diseases. For the classification and differentiation of centrifugally filtered HBV, HCV, and control serum samples, Principal component analysis is found helpful. Moreover, PLS-DA can classify these two distinct sets of SERS spectral data with 0.90 percent specificity, 0.85 percent precision, and 0.83 percent accuracy.
Conclusions: Surface enhanced Raman spectroscopy along with chemometric analysis like PCA and PLS-DA have been successfully differentiated HBV and HCV and healthy individuals' serum samples.

** Corresponding authors at: Department of Chemistry, University of Agriculture Faisalabad, Faisalabad 38000, Pakistan.
* Corresponding author at: Department of Chemistry, University of Education, Faisalabad Campus, Faisalabad 38000, Pakistan.
E-mail addresses: haqchemist@yahoo.com (H. Nawaz), irfan.majeed@uaf.edu.pk (M.I. Majeed), nosheenrasheed@yahoo.com (N. Rashid).

https://doi.org/10.1016/j.pdpdt.2023.103532
Received 9 December 2022; Received in revised form 13 March 2023; Accepted 21 March 2023
Available online 22 March 2023
1572-1000/© 2023 Elsevier B.V. All rights reserved.

1. Introduction

Hepatitis is the inflammation of liver which may occur due to virus attack which can range from A to E [1–3]. Hepatitis B and C are very chronic which cause permanent liver failure. Approximately 170 million population is chronically infected worldwide every year [3,4]. Hepatitis B and C are caused by viruses B (DNA virus) and C (RNA virus) respectively which are transmitted from one patient to other due to sharing of needles or other equipment which was already used and by transfer of body fluids. Initially, both diseases are asymptomatic and their symptoms are mostly same which usually appear at the chronic level. Fatigue, fever, poor appetite, nausea, abdominal pain, yellowing of eyes and skin, and diarrhea are the major symptoms of HBV and HCV [5]. The prolonged acute infection leads to hepatocellular carcinoma and liver cirrhosis which ultimately can cause death [6]. Different gold standard techniques are available for the diagnosis of these two closely related diseases. Enzyme Linked Immunosorbent Assay (ELISA) is done by using serum and saliva samples but considered expensive as it involve expensive consumables and antibody instability may lead to false positive and false negative results [7,8]. Liver biopsies would lead to bleeding, damage to neighboring tissues and can lead to cancer [9]. Liver function test uses Aspartate aminotransferase (AST) for disease diagnosis but can result abnormal values due to muscle injury which also causes increased AST value [10]. The HBV and HCV inside the host body can also be detected through polymerase chain reaction (PCR) which is a gold standard technique. However, these techniques have some loops like they have false negative and false positive results, need of skilled person, highly expensive instruments and time consuming [11].

Surface-enhanced Raman spectroscopy (SERS) as compared to normal Raman spectroscopy has a great capability to be used as analytical tool especially for the diagnosis of body fluids for disease diagnosis. Normal Raman spectroscopy can be employed for the diagnosis of biological samples which has been performed previously in the literature including prediction of viral loads for diagnosis of Hepatitis C infection in human plasma samples [12], analysis for screening of dengue infection [13] and for screening of Hepatitis C infection [14]. Moreover, in order to further improve the capability of Raman spectroscopy for analysis of biological samples, surface-enhanced Raman spectroscopy (SERS) is performed [15–17]. SERS is nondestructive nature, less time consuming and cheap as compare to other techniques [1,5,18–20].

The blood serum contains different proteins except fibrinogen [21]. Biomedical applications of SERS for the examination of serum samples of various diseases are reported including breast cancer [22] hepatitis B and C [18,23], dengue [22], typhoid [24], tuberculosis [24].

SERS has been used for the diagnosis of serum samples of HBV is reported for the viral loads prediction of HBV infection by employing chemometrics analysis like PLSR (Partial Least Square Regression Analysis) model [18,20]. Batool et al., reported that SERS is an excellent analytical tool for diagnosing and differentiating PCR products of Hepatitis C and Hepatitis B virus on the basis of their specific SERS spectral features [1].

For the analysis of blood serum samples, different kDa sizes centrifugal filters are used for the separation of proteins on density base from the serum [25,26] which can result into filtrate and residual parts. These separated parts of whole serum can be analyzed by SERS more effectively as there will be no interference of the bigger proteins in the signals of SERS. The current study is focused on the comparison of SERS spectral data sets of centrifugally filtrate portions of HBV and HCV serum diseases to establish a diagnostic method which potentially can give better results for the diagnosis of these viral diseases. To the best of our knowledge, still there is no literature has been reported which describes use of centrifugal filtration of the serum samples of HBV and HCV for the SERS analysis and their comparison. This can lead to develop SERS based diagnostic tools which can be rapid and cost effective as compared to conventional gold standard techniques.

HBV proteins come in a variety of forms, including core, surface, structural, and non-structural proteins. Most HBV proteins have sizes between 10 and 49 kDa, including the structural and non-structural proteins (24, 27, 39, 42 protein and 46 kDa) as well as the core proteins (15 and 17 kDa) and surface proteins (24 and 27 kDa) [27]. Moreover, important HCV proteins which are below the size of 50 kDa including capsid protein C (21 kDa), E1 (31 kDa), NS2 (23 kDa), NS4A (8 kDa), NS4B (27 kDa) [28]. Due to the above-mentioned sizes of the proteins of HBV and HCV, 50 kDa filter size was used for centrifugal filtration in order to eliminate the proteins bigger in size than this filter. Surface-enhanced Raman spectroscopy (SERS) is utilized to examine the filtrate parts of blood serum samples from HBV and HCV patients produced using centrifugal filters that have a 50 kDa pore size. As a result, the filtrate parts of the serum samples include proteins smaller than 50 kDa, and the elimination of larger size proteins makes it possible to more effectively acquire SERS spectrum [29].

2. Methodology

2.1. Preparation of Ag NPs

Chemical reduction method has been used for the preparation of silver nanoparticles which were used as a SERS substrate in data acquisition. The protocol of the synthesis of silver nanoparticles is reported in recent research paper [30]. Ag NPs were characterize through scanning electron microscopy (SEM) and their results shows that they are spherical in shape having diameter is 53 nm which is describe in previously published article [31].

2.2. Sample collection

Clinically isolated blood serum samples of HBV and HCV were collected from PINUM hospital, Faisalabad, Pakistan. Sample were prepared by using centrifugal filter membrane of 50 kDa by stirring at 1300 rpm. First of all, comparative analysis of controlled centrifuged serum samples is done with centrifuged serum samples of HBV and HCV of infected patients, Hepatitis B and Hepatitis C centrifuged serum samples were compared. In total 54 serum samples were collected including 22 serum samples of HBV, 22 serum samples of HCV and the remaining were healthy individual samples.

2.3. Centrifugal filtration

Centrifugal devices (Merck, Millipore) like Amicon Ultra-2 ml were employed for the centrifugation of serum samples of Hepatitis B, Hepatitis C and healthy samples having cutoff point of 50 kDa. For centrifugation of serum samples, 500 μL serum sample was transferred to filtration tube and centrifuge for 30 min at 6500 rpm. Two fractions were obtained after centrifugal filtration, one having high molecular weight fraction (HMWF) and the other is low molecular weight fraction (LMWF). High molecular weight fraction (molecular weight $>$ 50 kDa) called residue while low molecular weight fraction (molecular weight $<$ 50 kDa) called filtrate. These two fractions of all serum samples were transferred in a separate vials and stored in a fridge till SERS acquisition [32].

2.4. SERS data acquisition

Optosky Raman spectrometer (ATR8300BS) were employed to collect all the spectral data of serum samples with a 785 nm diode laser as an excitation source, 40X objective with the laser power of 100 mW and 2 s integration time. For SERS acquisition, 50 μl of filtrate serum sample and 50 μl of Ag NPs were incubated in an eppendorf for 30 min to make effective interaction. 50 μl of incubated sample was transferred on a small groove of aluminum slide, focused with 40X objective, 100 mW laser light and integration time of 2 s to record SERS spectral data of

each sample. All these conditions were kept same to ensure the reproducibility of our samples.

2.5. Preprocessing of SERS spectral data

MATLAB 7.8 version is a statistical software which was used to preprocess the all collected raw data of HBV, HCV and healthy serum samples. Raw data contain useful information but it also has noise and some spikes. All the raw data were combined into a single matrix to remove unwanted information and collect useful information by doing baseline correction, smoothing, vector normalization and substrate removal. Smoothing is done with the Savitzky-Golay algorithm while baseline correction is done with rubber band and polynomial method. In one matrix, spectral data sets of all the samples went through the same preprocessing. Table 1 shows the peak assignments for SERS spectral data. All the samples including HBV, HCV and healthy serum samples were differentiated and classify through Chemometric analysis like PCA (Principal Component Analysis) and PLS-DA (Partial Least Square Discriminant Analysis).

Principal component analysis is chemometric analysis used to assess variability and differentiation of spectral data sets as well as reasons for their differentiation into classes. PCA works by reducing the dimensionality of large data, minimize the loss of information while variability remain intact [33]. PLS-DA is a simple and effective method for identifying discriminative features for classification prediction and verifying classification validity. PLS-DA is an useful approach that may be employed to spectral data for prediction, validation, descriptive modeling and data splitting into different sets to characterize disease on different stages [34].

Table 1
SERS peak assignment of spectral features of HBV, HCV and healthy centrifugal filtered serum samples.

Peak position	Peak Assignments	References
529cm^{-1}	Uracil	[35,36]
583cm^{-1}	Out of plane bending of OH	[37]
589cm^{-1}	v4 $PO4^{3-}$ Symmetric stretching vibration	[38]
621cm^{-1}	Thymine	[39]
638cm^{-1}	Methionine	[24,40-42]
678cm^{-1}	DNA bases (Ring breathing modes), G C-2-endo anti/ (ring breathing)	[27,43]
729cm^{-1}	Adenine (RNA/DNA)	[27,42,44, 45]
748cm^{-1}	Adenine in RNA/DNA	[46]
786cm^{-1}	Uracil	[42,47]
810cm^{-1}	Phosphodiester (Z-marker)	[43]
840cm^{-1}	Alpha-Anomers Glucose-saccharide band	[36,48]
853cm^{-1}	Proline/Tyrosine	[27,47,49]
880cm^{-1}	Tryptophan, sigma(ring)	[46]
950cm^{-1}	Stretching of amino acids, proline, valine and polysaccharides	[27,50]
1014cm^{-1}	N-sugar stretching mode of thymine	[36,51]
1073 cm^{-1}	Triglyceride (HBV)	[52]
1073 cm^{-1}	DNA content in cell (HCV)	[53,54]
1099cm^{-1}	v(C—N)	[27,38]
1131cm^{-1}	Fatty acid	[27,55]
1208 cm^{-1}	Phenylalanine	[55]
1280cm^{-1}	Phosphates and Nucleic acids	[56,57]
1319cm^{-1}	B, Z-marker of Guanine	[58]
1336cm^{-1}	Guanine	[27,58]
1373cm^{-1}	Guanine (DNA/RAN bases)	[43,59]
1395cm^{-1}	Thymine	[60]
1417cm^{-1}	Quinoid ring stretching (C = C)	[61,62]
1446cm^{-1}	CH_2 proteins bending mode	[47]
	CH_2 defor	[27,45]
1540cm^{-1}	Aromatic hydrogen, amide group vibrations and carbonyl group vibrations	[36,63]
1588cm^{-1}	Phenylalanine, Hydroxyproline	[27,38]
1674cm^{-1}	C = C stretch vibration	[64]

3. Results

Transmission electron microscopy (TEM) was used to examine silver nanoparticles which confirmed that Ag NPs had an oval geometry and size of 53 nm as published elsewhere [19]. According to studies, nanoparticles in this size range have high SERS activity.

3.1. Mean plot of HBV, HCV and control filtrate

SERS mean spectra of filtrate portions of the serum samples collected by centrifugal filters of 50 kDa size as HBV disease (green spectra), HCV disease (red spectra) and true healthy samples (black spectra) are shown in Fig. 1. DNA is corresponding to hepatitis B while RNA is corresponding to hepatitis C disease with respect to the type of their virus. Notably, major difference between RNA and DNA is that RNA has the uracil nucleobase while DNA has thymine base. The SERS peak at 786 cm^{-1} assigned to Uracil base [36] is present in centrifugally filtered HCV serum sample (HCV is RNA virus) and absent in centrifugally filtered HBV filtrate serum. On the other hand, the SERS peaks observed at 621 cm^{-1} (thymine) [39] and 1014 cm^{-1} (thymine) [1,65] in centrifugally filtered HBV serum samples (HBV is DNA virus) while absent in healthy and centrifugally filtered HCV serum. This information helps to differentiate infection caused by two different viruses including hepatitis B which is DNA and hepatitis C which is RNA virus.

The differentiating SERS spectral features are denoted with solid lines and dashed lines. The features labelled with solid lines are linked with the solely observed SERS spectral differences in any sample and dotted lines are related to the intensities-based SERS spectral differences. The SERS bands are only observed in the filtrate portions of the serum samples of clinically diagnosed HCV patients include 621, 678, 786, 810, 840, 853, 880, 950, 1260, 1319, and 1540 cm^{-1}. Centrifugally filtered serum of control and HCV samples have some common SERS band in filtrate portion like 529, 589, 853, 950, 1073, 1417, and 1674 cm^{-1}. SERS bands which are common in filtrates of serum of HBV and HCV samples appear at 548, 583, 748, 1099, 1336, 1373, 1446 and 1588 cm^{-1}. Moreover, the SERS bands that are commonly present in centrifuged healthy, HBV and HCV diagnosed serum samples appear at 583, 728, 748, 1099, 1336, 1446, and 1588 cm^{-1}.

3.2. Multivariate data analysis techniques

3.2.1. Principal component analysis (PCA)

Chemometric analysis like principal component analysis (PCA) has been employed on the SERS processed data sets of filtrate portions obtained by centrifugal filters of 50 kDa size for 10 control serum samples, 22 HBV serum samples and 22 HCV serum samples.

Fig. 2 depicts the overall scatter score of centrifugally filtered serum of HBV, HCV and control serum sample. The PC-1 shows 67% variability while PC-2 shows 36% variability in the SERS spectral data sets. Diseases classes are denoted by red dots and green dots which are clustered on the positive side of x-axis while controlled samples are denoted by block dots which are present on negative side of x-axis. HBV filtrate are represented by green dots, HCV filtrate samples represented by red dots and black dots represent the control filtrate sample serum. Diseases classes are clustered on one side showing resemblance and show clear difference from healthy class which is clustered on negative side of the x-axis. This PCA scatter plot shows clear difference between healthy, HBV and HCV serum sample on the basis of their biochemical features.

In order to identify the biochemical differences between HBV and HCV filtrate serum, a pair wise PCA analysis is done to compare these two groups. Fig. 3(a) shows the scatter score plot between HBV and HCV serum filtrate samples having PC-1 exhibits 37% while PC-2 value is 23% variability. Furthermore, green color dots are clustered on the negative side of the scatter plot represent the SERS spectra of centrifugally filtered HBV serum samples, while red color dots are grouped on the positive side represent the HCV filtered serum of spectral data. Fig. 3

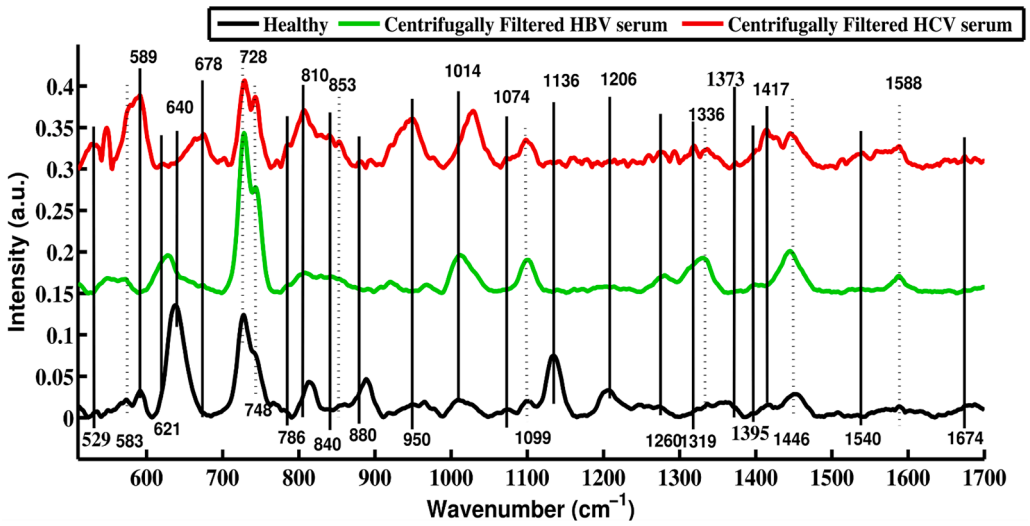

Fig. 1. Mean SERS spectra of filtrate portions of HBV, HCV and healthy serum samples. Solid lines represent the differences and dotted lines represent the similarities.

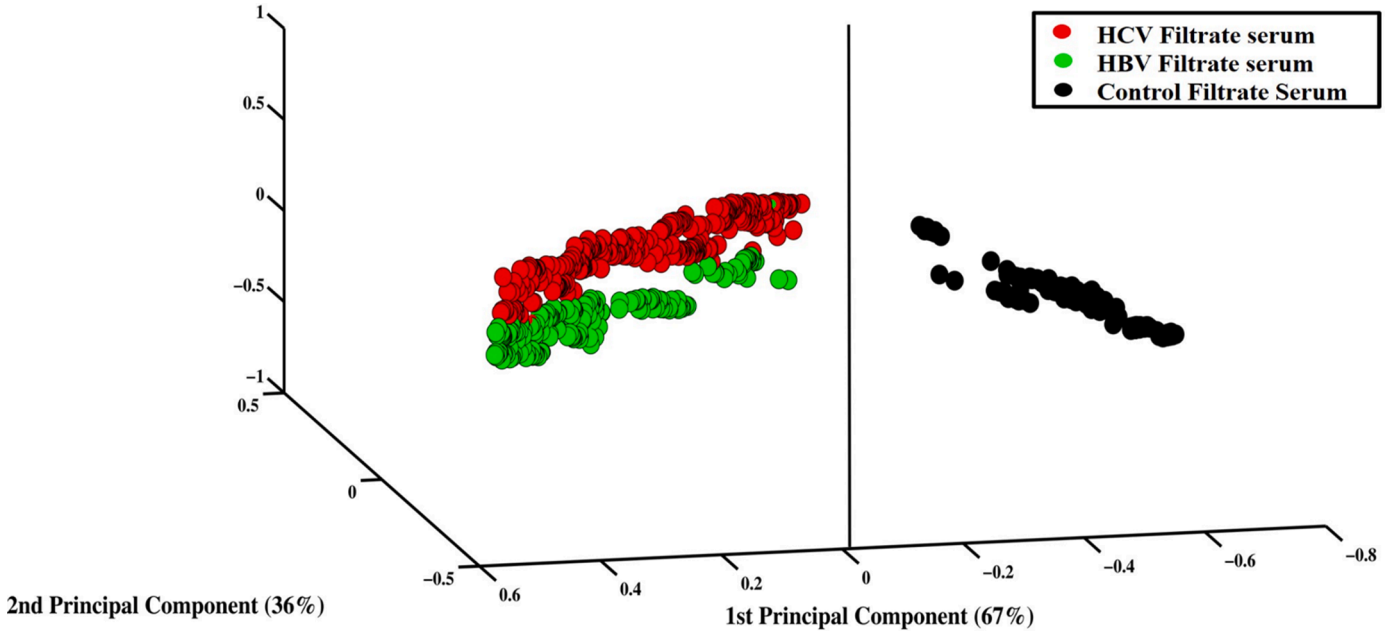

Fig. 2. Combined PCA score plot of the SERS spectral data sets of filtrate portions of HBV, HCV and healthy serum samples.

(b) shows PCA loadings between HBV and HCV filtrate serum sample. The positive loadings which are linked with HCV serum are 529,583, 589, 748, 950, 1131, 1294, 1319,1336, 1373 and 1395 cm^{-1}. Furthermore, the negative loadings are linked with spectral data of filtrate portions of HBV serum samples including 621, 640, 678, 786, 810, 840, 853, 880, 1014, 1073, 1099, 1280, 1446, 1540, 1588 and 1674 cm^{-1}. These biomarkers are helpful in differentiating between HBV and HCV filtrate serum on the basis of biochemical compositions associated with two diseases.

3.2.2. *Partial least square discriminant analysis (PLS-DA)*

PLS-DA is a supervised method which is used for the quantitative differentiation between HBV and HCV centrifugally filtrate serum samples having 50 kDa size. In this case, 40% of the data is used to calibrate the model and determine the number of latent variables, while 60% of the data is utilized to validate the model. There was a total of 15 latent variables found optimum for development of the model. In Fig. 4 SERS spectral of filtrate portions of HBV serum samples (green dots) are grouped on the negative side of the score plot, while those of HCV serum samples (red dots) are clustered on the positive side of the score plot. The PLS-DA score plot clearly distinguishes SERS spectral data sets of filtrate portions between HBV and HCV serum samples. Fig. 5 shows the developed PLS-DA model which has shown 0.90 percent specificity, 0.85 percent precision and 0.83 percent accuracy. These parameters suggest that PLS-DA model is found effective for the classification of the SERS spectral data sets of two different viral diseases. The Receiver operating characteristic curve (ROC) depicts model cross validation and area under the curve (AUC) value near 1 indicates that the model is accurate, whereas a value of zero indicates that model is invalid. Fig. 5 shows the ROC curve of PLS-DA model of SERS spectral data of HBV and HCV and obtained value of the AUC curve 0.71, which is close to 1 indicating that the model is best fit and produces excellent differentiation results.

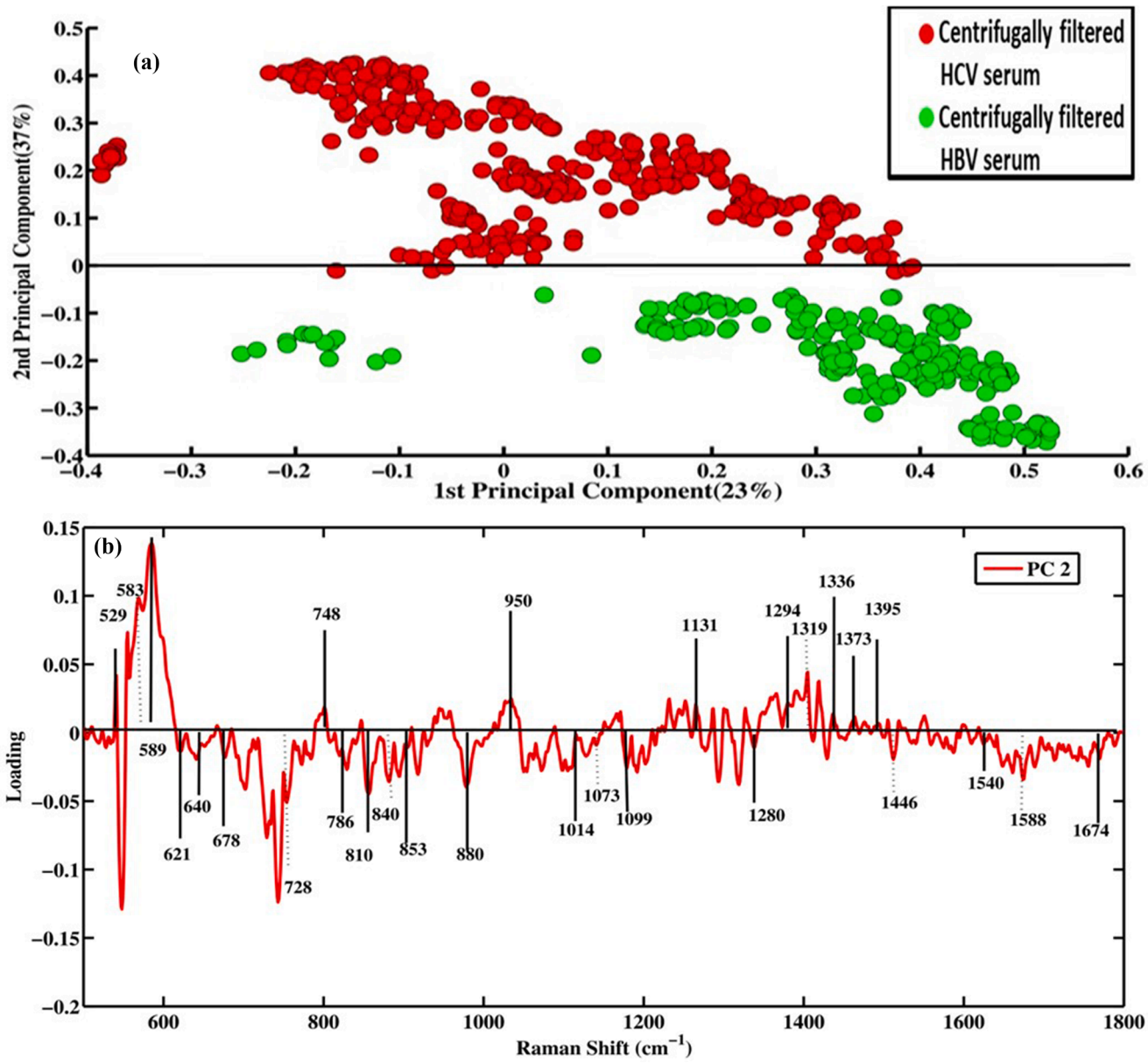

Fig. 3. Principal component analysis score plot of SERS spectral data sets of filtrate portions of HCV serum (red) and HBV (green) serum samples (a) and loadings of PCA (b).

4. Discussion

In comparison to their uncentrifuged/whole serum, the hepatitis B disease biomarkers are more apparent after centrifugation. Centrifugally filtered blood samples of hepatitis B were easily distinguished from centrifugally filtered serum samples of healthy people using statistical techniques including principal component analysis (PCA) and partial least square discriminant analysis (PLS-DA). Centrifugal filtration method is also used to examine the qualitative and quantitative analysis of HCV serum samples which can potentially give more accurate results for the diagnosis of hepatitis C. In order to analyze the filtrate parts of the serum samples of HCV patients obtained by employing centrifugal filters of 50 kDa, surface-enhanced Raman spectroscopy (SERS) is used. As a result, the filtrate portion of the serum samples contain proteins smaller than 50 kDa, and the elimination of larger size proteins makes it possible to more effectively acquire SERS spectral features of smaller proteins, which are likely linked to Hepatitis C disease.

The differentiating SERS bands present in SERS mean spectrum of hepatitis C are observed at 529, 639, 678, 856, 945, 1014,1102, 1131,1332 and 1374 cm^{-1} which are found in previously published work [36,65]. The differentiating SERS bands of hepatitis B are observed at 841, 853, 950, 1099, 1131, 1136, 1446, 1540 and 1588 cm^{-1} which are observed in previously published work [27,54]. The differentiating SERS spectral bands as mentioned in Fig. 1, The peak at 1373 cm^{-1} (DNA/RNA bases) is found with enhanced peak intensity and due to increased contents of RNA in HBV and HCV positive filtrate portion of serum as compared to healthy sample. The prominent SERS features of phosphate group appears at 589 and 810 cm^{-1} which are found in both DNA and RNA and at position 589 cm^{-1} no peak is found in HBV but it shows slight shift towards higher wave number in RNA spectra. The SERS features at 1014 and 1395 cm^{-1} are associated with thymine and are only present in mean SERS spectrum of filtrate portion of HBV serum. Notably, as thymine is a DNA base hence these peaks are only observed in the mean spectrum of HBV (DNA based virus) positive samples and absent in HCV (RNA virus) positive samples. On the similar basis, the features of Uracil which is a RNA nitrogenous base, are

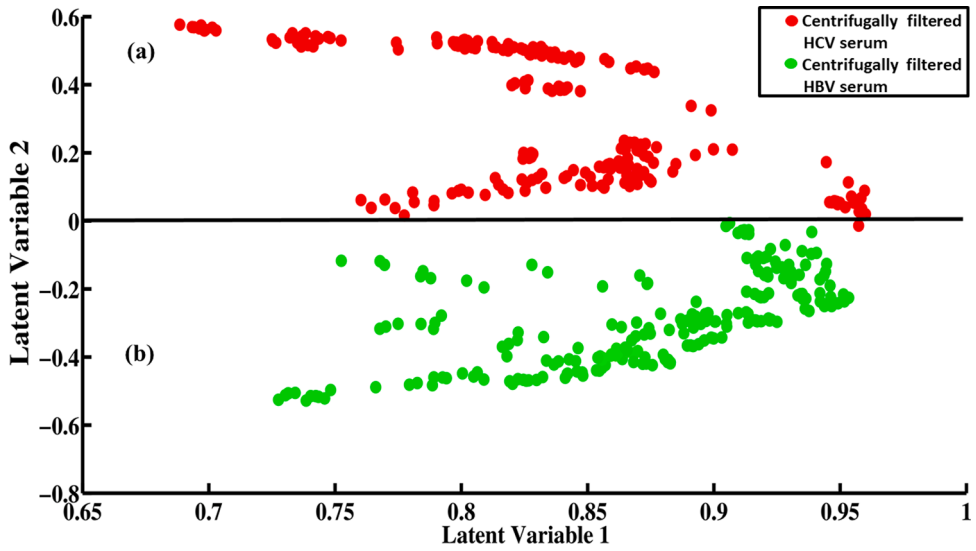

Fig. 4. PLS-DA Scatter diagram of SERS spectral data sets of filtrate portions of HBV (green) and HCV (red) serum samples.

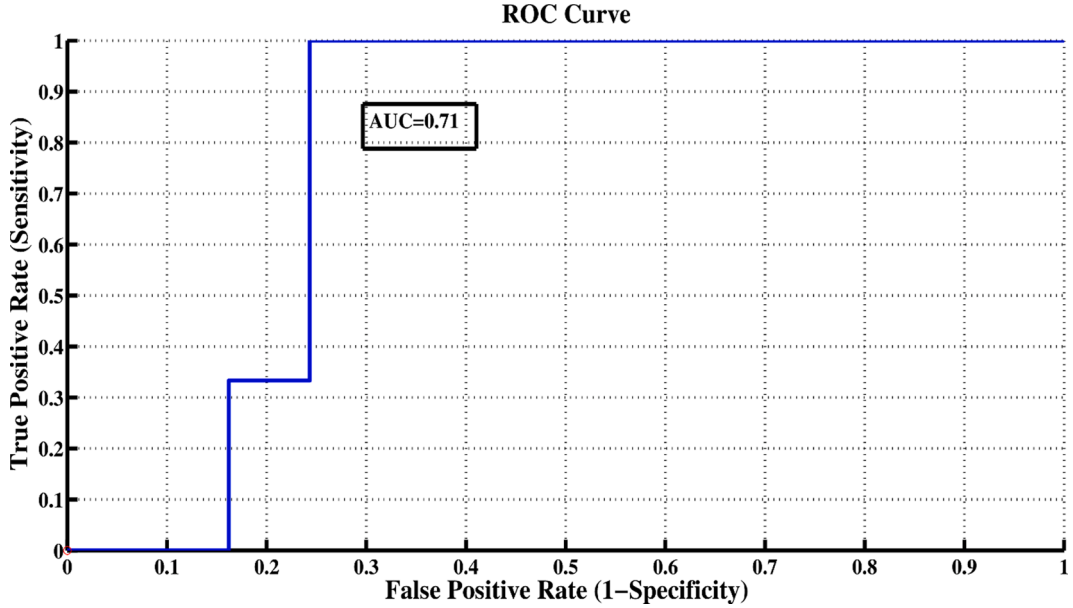

Fig. 5. Receiver operating characteristic curve (ROC) of PLS-DA SERS spectral data set of HBV, HCV and control serum sample.

observed only in HCV positive samples at positions 529 cm^{-1}(ring stretching of uracil) and 786 cm^{-1}(pyridine ring breathing mode of uracil). The peaks appearing at 729 cm^{-1} (adenine) and 748 cm^{-1} (adenine) with increased peak intensity is found in filtrate portions of both HBV and HCV serum spectra as compared to control serum spectra due to contents of DNA/RNA in the form of adenine in both HBV and HCV. The peak appearing at 853 cm^{-1}(ring breathing mode of Tyrosine) is observed in HCV and HBV as well healthy samples. The SERS features of carbohydrates appearing at 840 cm^{-1}(glucose saccharide band) and 950 cm^{-1}(polysaccharides). The peak intensity at position 840 and 950 cm^{-1} is increased in HCV serum spectra but absent in HBV serum spectra at this position. The features of proteins appear at 1446 cm^{-1}. The peak intensity at 1260cm^{-1}(Amide III band) and 1446 cm^{-1}(CH_2 bending mode of proteins) is increased in both HBV and HCV serum spectra as compared to control serum spectra hence may be due to the proteins directly related to the both viruses of HBV and HCV. Other peaks related to proteins appear at 621 and 1588 cm^{-1} and are found with increased peak intensity in both HBV and HCV due to HBV and HCV viral infection. The SERS peak appears at 1099 cm^{-1} (C—N stretching) and 880 cm^{-1} (tryptophan)with increased peak intensity in both HBV and HCV serum spectra due to increased contents of proteins as compared to healthy samples. One peak appears at 1540 cm^{-1} which is slightly higher in HCV as compared to control spectra and absent in HBV due to amide carbonyl group vibration and aromatic hydrogen. The SERRS peak appears at 638 cm^{-1} which is present in healthy filtrate but absent in both HBV and HCV filtrate due to presence of methionine. Low concentration of methionine can also lead to the cell proliferation and cell morphological changes. The peak appears at 1073 cm^{-1} is absent in HBV due to increased concentration of Triglycerides and increased in HCV due to increased content of DNA in the cell. The peak at 1135 cm^{-1} is observed in normal serum samples but absent in HBV and HCV filtrate due to presence of fatty acids and one peak appear at 1208 cm^{-1} is absent in both HBV and HCV but present in healthy serum samples due to phenylalanine. The peak appearing at 1417 cm^{-1} is due to quinoid ring which is increased in HCV than normal serum samples but absent in HBV. J-Nagakawa was studied in galactosamine-induced hepatitis

model in F344 rats in which endogenous endotoxin is believed to play a critical pathogenic role [62].

5. Conclusions

The disease biomarkers present in centrifuged serum samples are found more prominent as compared to uncentrifuged serum samples employing centrifugal filters of 50 kDa. The blood serum samples of hepatitis B and C centrifuged by using centrifugally filtered devices were easily distinguished from centrifugally filtered serum samples of healthy people by using principal component analysis (PCA) and partial least square discriminant analysis (PLA-DA). Hepatitis B and C diagnosis may be improved by using the centrifugal filtration method to evaluate the qualitative and quantitative analyses of HBV and HCV serum samples. SERS along with chemometric analysis like PCA and PLS-DA is an effective in identifying the biochemical features of HBV and HCV diseases in the form of SERS spectral peaks of centrifugal filtration of the serum samples. Moreover, this approaches also found very useful for comparing two different diseases with almost identical symptoms. This helps the differentiation of the two diseases based on biochemical differences. Many distinguishing SERS spectral features including 529, 589, 678, 810, 950, and 1540 cm^{-1} are identified by the comparison of the HBV and HCV SERS spectral data sets. PCA analysis is found helpful for differentiation between the SERS spectral data sets of the HBV, HCV and healthy/control serum samples. The PLS-DA analysis was used to verify the authenticity of SERS spectral data classification for two diseases with 0.90 percent specificity, 0.85 percent precision and 0.83 percent accuracy.

Funding information

This research did not receive any specific grant from funding agencies in the public, commercial, or not-for-profit sectors.

CRediT authorship contribution statement

Muhammad Zaman Nawaz: Writing – original draft. **Haq Nawaz:** Project administration. **Muhammad Irfan Majeed:** Supervision. **Nosheen Rashid:** Validation. **Muhammad Rizwan Javed:** Investigation. **Saima Naz:** Investigation. **Muhammad Zeeshan Ali:** Visualization. **Amina Sabir:** Methodology. **Nimra Sadaf:** Data curation. **Ali Raza:** Formal analysis. **Muhammad Shakeel:** Writing – review & editing. **Zain Ali:** Visualization. **Imran Amin:** Resources.

Declaration of Competing Interest

The authors have no known competing financial interests or personal relationships that could have appeared to influence the work reported in this paper.

References

[1] F. Batool, et al., Surface-enhanced Raman spectral analysis for comparison of PCR products of hepatitis B and hepatitis C, Photodiagnosis Photodyn. Ther. 35 (2021), 102440.
[2] C.M.M.D. Cordova, et al., Determination of capillary blood glucose and venous blood glucose with a glucometer versus laboratory determination of venous plasma glucose, J. Bras. Patol. Med. Lab. 45 (5) (2009) 378–384.
[3] R.D.C.F. Borges, et al., Detecting alterations of glucose and lipid components in human serum by near-infrared Raman spectroscopy, Res. Biomed. Eng. 31 (2) (2015) 160–168.
[4] S. Blach, et al., Global prevalence and genotype distribution of hepatitis C virus infection in 2015: a modelling study, Lancet Gastroenterol. Hepatol. 2 (3) (2017) 161–176.
[5] S. Rafiq, et al., Surface-enhanced Raman spectroscopy for analysis of PCR products of viral RNA of hepatitis C patients, Spectrochim. Acta A 259 (2021) 119908.
[6] L.J. de Oliveria Andrade, et al., Association between hepatitis C and hepatocellular carcinoma, J. Glob. Infect. Dis. 1 (1) (2009) 33.
[7] A. Garritsen, et al., Two-tiered SARS-CoV-2 seroconversion screening in the Netherlands and stability of nucleocapsid, spike protein domain 1 and neutralizing antibodies, Infect. Dis. 53 (7) (2021) 498–512.
[8] L. Katz, et al., Performance of an algorithm for the reentry of volunteer blood donors deferred due to false-positive test results for antibody to hepatitis B core antigen, Transfusion 48 (11) (2008) 2315–2322.
[9] E.H.J.R. Smith, Complications of percutaneous abdominal fine-needle biopsy, Review 178 (1) (1991) 253–258.
[10] G. ArAGon, Z.M. Younossi, When and how to evaluate mildly elevated liver enzymes in apparently healthy patients, Clevel. Clin. J. Med. 77 (3) (2010) 195–204.
[11] R.W. Chen, et al., Real-time PCR for detection and quantitation of hepatitis B virus DNA, J. Med. Virol. 65 (2) (2001) 250–256.
[12] H. Nawaz, et al., Prediction of viral loads for diagnosis of Hepatitis C infection in human plasma samples using Raman spectroscopy coupled with partial least squares regression analysis, J. Raman Spectrosc. 48 (5) (2017) 697–704.
[13] T. Mahmood, et al., Raman spectral analysis for rapid screening of dengue infection, Spectrochim. Acta Part A 200 (2018) 136–142.
[14] A. Ditta, et al., Principal components analysis of Raman spectral data for screening of Hepatitis C infection, Spectrochim. Acta Part A 221 (2019), 117173.
[15] R.Z.A. Bari, et al., Surface-enhanced Raman spectroscopic analysis of centrifugally filtered HBV serum samples, Photodiagnosis Photodyn. Ther. 38 (2022), 102808.
[16] M. Akram, et al., Surface-enhanced Raman spectroscopy for characterization of filtrate portions of blood serum samples of typhoid patients, Photodiagnosis Photodyn. Ther. 40 (2022), 103199.
[17] U. Ehsan, et al., Surface-enhanced Raman spectroscopy of centrifuged blood serum samples of diabetic type II patients by using 50 KDa filter devices, Spectrochim. Acta Part A 293 (2023), 122457.
[18] S. Ahmad, et al., Characterization and prediction of viral loads of Hepatitis B serum samples by using surface-enhance Raman spectroscopy (SERS), Photodiagnosis Photodyn. Ther. 35 (2021), 102386.
[19] M. Kashif, et al., Surface Enhanced Raman Spectroscopy of the serum samples for the diagnosis of Hepatitis C and prediction of the viral loads, Spectrochim. Acta A 242 (2020) 118729.
[20] S. Tabbasum, et al., Surface-enhanced Raman spectroscopy for comparison of serum samples of typhoid and tuberculosis patients of different stages, Photodiagnosis Photodyn. Ther. 35 (2021), 102426.
[21] S. Herrick, et al., Fibrinogen, Int. J. Biochem. Cell Biol. 31 (7) (1999) 741–746.
[22] H. Nargis, et al., Comparison of surface enhanced Raman spectroscopy and Raman spectroscopy for the detection of breast cancer based on serum samples, Spectrochim. Acta A 246 (2021), 119034.
[23] S. Nasir, et al., Surface enhanced Raman spectroscopy of RNA samples extracted from blood of hepatitis C patients for quantification of viral loads, Photodiagnosis Photodyn. Ther. 33 (2021) 102152.
[24] M. Tahira, et al., Surface-enhanced Raman spectroscopy analysis of serum samples of typhoid patients of different stages, Photodiagnosis Photodyn. Ther. 34 (2021), 102329.
[25] F. Bonnier, M.J. Baker, H.J.J.A.M. Byrne, Vibrational spectroscopic analysis of body fluids: avoiding molecular contamination using centrifugal filtration, Anal. Methods 6 (14) (2014) 5155–5160.
[26] D.R. Parachalil, et al., Raman spectroscopic screening of high and low molecular weight fractions of human serum, Analyst 144 (14) (2019) 4295–4311.
[27] R.Z.A. Bari, et al., Surface-enhanced Raman spectroscopic analysis of centrifugally filtered HBV serum samples, Photodiagnosis Photodyn. Ther. 38 (2022), 102808.
[28] A. Grakoui, et al., Expression and identification of hepatitis C virus polyprotein cleavage products, J. Virol. 67 (3) (1993) 1385–1395.
[29] S. Shakeel, et al., Surface-enhanced Raman spectroscopic analysis of centrifugally filtered blood serum samples of hepatitis C patients, Photodiagnosis Photodyn. Ther. 39 (2022), 102949.
[30] M. Shakeel, et al., Surface-enhanced Raman spectroscopy for the characterization of pellets of biofilm forming bacterial strains of Staphylococcus epidermidis, Photodiagnosis Photodyn. Ther. 40 (2022) 103145.
[31] M. Kashif, et al., Surface enhanced Raman Spectroscopy of the serum samples for the diagnosis of Hepatitis C and prediction of the viral loads, Spectrochim. Acta Part A 242 (2020), 118729.
[32] F. Bonnier, et al., Screening the low molecular weight fraction of human serum using ATR-IR spectroscopy, J. Biophotonics 9 (10) (2016) 1085–1097.
[33] S.Y. Liu, et al., Human liver tissue metabolic profiling research on hepatitis B virus-related hepatocellular carcinoma, World J. Gastroenterol. 19 (22) (2013) 3423.
[34] L.C. Lee, C.Y. Liong, A.A. Jemain, Partial least squares-discriminant analysis (PLS-DA) for classification of high-dimensional (HD) data: a review of contemporary practice strategies and knowledge gaps, Analyst 143 (15) (2018) 3526–3539.
[35] J. De Gelder, et al., Reference database of Raman spectra of biological molecules, J. Raman Spectrosc. Int. J. Orig. Work Asp. Raman Spectrosc. Incl. High. Order Process. Brillouin Rayleigh Scatt. 38 (9) (2007) 1133–1147.
[36] F. Batool, et al., Surface-enhanced Raman spectral analysis for comparison of PCR products of hepatitis B and hepatitis C, Photodiagnosis Photodyn. Ther. 35 (2021) 102440.
[37] H. Schulz, M. Baranska, Identification and quantification of valuable plant substances by IR and Raman spectroscopy, Vib. Spectrosc. 43 (1) (2007) 13–25.
[38] W.T. Cheng, et al., Micro-Raman spectroscopy used to identify and grade human skin pilomatrixoma, Microsc. Res. Tech. 68 (2) (2005) 75–79.
[39] L. Qiu, et al., Analysis of plant genomic DNAs and the genetic relationship among plants by using surface-enhanced Raman spectroscopy, Vib. Spectrosc. 72 (2014) 134–141.

[40] G. Shetty, et al., Raman spectroscopy: elucidation of biochemical changes in carcinogenesis of oesophagus, Br. J. Cancer 94 (10) (2006) 1460–1464.
[41] S.J. Mentch, et al., Histone methylation dynamics and gene regulation occur through the sensing of one-carbon metabolism, Cell Metab. 22 (5) (2015) 861–873.
[42] S. Shakeel, et al., Surface-enhanced Raman spectroscopic analysis of centrifugally filtered blood serum samples of hepatitis C patients, Photodiagnosis Photodyn. Ther. 39 (2022), 102949.
[43] J.W. Chan, et al., Micro-Raman spectroscopy detects individual neoplastic and normal hematopoietic cells, Biophys. J. 90 (2) (2006) 648–656.
[44] Z. Liu, et al., Circulation and long-term fate of functionalized, biocompatible single-walled carbon nanotubes in mice probed by Raman spectroscopy. 2008. 105 (5): p. 1410–1415.
[45] C.J. Frank, R.L. McCreery, D.C. Redd, Raman spectroscopy of normal and diseased human breast tissues, Anal. Chem. 67 (5) (1995) 777–783.
[46] J. Binoy, et al., NIR-FT Raman and FT-IR spectral studies and ab initio calculations of the anti-cancer drug combretastatin-A4, J. Raman Spectrosc. 35 (11) (2004) 939–946.
[47] N. Stone, et al., Raman spectroscopy for identification of epithelial cancers, Faraday Discuss. 126 (2004) 141–157.
[48] R.J. Lakshmi, et al., Tissue Raman spectroscopy for the study of radiation damage: brain irradiation of mice, Radiat. Res. 157 (2) (2002) 175–182.
[49] N. Stone, et al., Near-infrared Raman spectroscopy for the classification of epithelial pre-cancers and cancers, J. Raman Spectrosc. 33 (7) (2002) 564–573.
[50] M. Gniadecka, et al., Diagnosis of basal cell carcinoma by Raman spectroscopy, J. Raman Spectrosc. 28 (2–3) (1997) 125–129.
[51] D. Lin-Vien, et al., The Handbook of Infrared and Raman characteristic Frequencies of Organic Molecules, Elsevier, 1991.
[52] L. Silveira Jr., et al., Correlation between near-infrared Raman spectroscopy and the histopathological analysis of atherosclerosis in human coronary arteries, Lasers Surg. Med. 30 (4) (2002) 290–297.
[53] L. Chiriboga, et al., Infrared spectroscopy of human tissue. I. differentiation and maturation of epithelial cells in the human cervix, Biospectroscopy 4 (1) (1998) 47–53.
[54] S. Ahmad, et al., Characterization and prediction of viral loads of Hepatitis B serum samples by using surface-enhanced Raman spectroscopy (SERS). Photodiagnosis Photodyn, Ther 35 (2021) 102386.
[55] Z. Huang, et al., Near-infrared Raman spectroscopy for optical diagnosis of lung cancer, Int. J. Cancer 107 (6) (2003) 1047–1052.
[56] P.G. Andrus, R.D.J.B. Strickland, Cancer grading by Fourier transform infrared spectroscopy, Biospectroscopy 4 (1) (1998) 37–46.
[57] Z. Movasaghi, S. Rehman, I.U. Rehman, Raman spectroscopy of biological tissues, Appl. Spectrosc. Rev. 42 (5) (2007) 493–541.
[58] A. Ruiz-Chica, et al., Characterization by Raman spectroscopy of conformational changes on guanine–cytosine and adenine–thymine oligonucleotides induced by aminooxy analogues of spermidine, J. Raman Spectrosc. 35 (2) (2004) 93–100.
[59] M. Kashif, et al., Surface-enhanced Raman spectroscopy for identification of food processing bacteria, Spectrochim. Acta Part A 261 (2021), 119989.
[60] K. Song, W. Kim, K. Nakata, Evaluation of microstructures and mechanical properties of friction stir welded lap joints of Inconel 600/SS 400, Mater. Des. 35 (2012) 126–132.
[61] J. Laska, J.J.P. Widlarz, Spectroscopic and structural characterization of low molecular weight fractions of polyaniline, Polymer 46 (5) (2005) 1485–1495.
[62] J. Nagakawa, et al., Protective effect of E3330, a novel quinone derivative, in galactosamine-induced hepatitis in rats, J. Pharmacol. Exp. Ther. 264 (1) (1993) 496–500.
[63] B.R. Wood, et al., FTIR microspectroscopic study of cell types and potential confounding variables in screening for cervical malignancies, Biospectroscopy 4 (2) (1998) 75–91.
[64] E.O. Faolain, et al., A study examining the effects of tissue processing on human tissue sections using vibrational spectroscopy, Vib. Spectrosc. 38 (1–2) (2005) 121–127.
[65] F. Batool, et al., SERS-based viral load quantification of hepatitis B virus from PCR products, Spectrochim. Acta Part A 255 (2021), 119722.